Level Set Based Shape Prior Segmentation

Tony Chan
Dept. of Mathematics
University of California, Los Angeles
TonyC@college.ucla.edu

Wei Zhu
Courant Institute of Mathematical Sciences
New York University
wzhu@cims.nyu.edu

Abstract

We propose a level set based variational approach that incorporates shape priors into Chan-Vese's model [3] for the shape prior segmentation problem. In our model, besides the level set function for segmentation, as in Cremers' work [5], we introduce another labelling level set function to indicate the regions on which the prior shape should be compared. Our model can segment an object, whose shape is similar to the given prior shape, from a background where there are several objects. Moreover, we provide a proof for a fast solution principle, which was mentioned [7] and similar to the one proposed in [19], for minimizing Chan-Vese's segmentation model without length term. We extend the principle to the minimization of our prescribed functionals.

1. Introduction

Image segmentation is a fundamental topic in image processing. Numerous approaches have been proposed for this problem. A fundamental variational approach is the use of the Mumford-Shah's functional which was discussed comprehensively in [13, 12]. In this approach, the segmentation problem is to find a piecewise smooth function which approximates the image and also prohibits the excessive length of the boundaries between any two contiguous regions. The methodology has brought forth lots of models on segmentation. A direct one is its modified model that approximates the Mumford-Shah's functional via $\Gamma-$ convergence [1] since it is difficult to handle the length of the boundaries. Later, in [3], Chan and Vese proposed a novel model that combines the Mumford-Shah's functional and level set methods [15], which can handle curves, surfaces with topological changes easily. Besides these models, in [8], Kass et. al. proposed the classic snake model for segmentation and Malladi et al. in [11], Caselles et al. in [2] developed their geodesic active contour models.

However, the above models are all gray intensity based.

They fail to segment meaningful objects from images when the objects are occluded by other objects or some parts of them are in low gray contrasts or even missing. In fact, these situations always happen in practical applications. Therefore, in these cases, $prior$ shape information is needed to successfully segment the desirable objects. The process of segmentation with the incorporation of shape information can be called $shape\ prior\ segmentation.$

There are also many works on shape prior segmentation in the literature [9, 10, 2, 4, 6, 20]. Almost all these works are linear combinations of two functionals with one about some specific segmentation functional and the other about shape difference. For example, in [9, 10], Leventon et. al. presented a model which incorporates statistical based shape information into Caselles' geometric active contours model [2]. Later, Chen et. al. [4] combined a different shape difference term with the same segmentation model. Moreover, in [6], Cremers et al. proposed a shape prior segmentation model which puts a statistical based shape prior into the Mumford-Shah's functional.

In a recent paper [5], Cremers et al. constructed a variational approach that incorporates a level set based shape difference term into Chan-Vese's segmentation model [3]. Besides the level set function for segmentation, the authors also introduced a labelling function to indicate the regions in which shape priors should be enforced.

In this paper, based on Chan-Vese's model, we propose a variational model for shape prior segmentation. In this model, we borrow the idea of Cremer et al's work in [5], i.e., we also introduce a labelling function. However, our model is different from Cremer's model in several aspects. Firstly, our approach allows translation, scaling and rotation of prior shapes, i.e, it can deal with the general case that the locations, sizes and poses of the desired objects are all unknowns. Secondly, we take a different shape comparison term which is intrinsic to the objects and the prior shapes, in other words, it is independent of the image domain. Moreover, we introduce additional terms to control the labelling function.

The rest of this paper is organized as follows. In sec-

tion 2, a shape representation via the related signed distance function is discussed. In section 3, we review Cremers et al's prior segmentation model [5]. Then, we detail our variational model in section 4. Section 5 contains the numerical algorithms, and the experimental results are presented in Section 6, which is followed by a conclusion in section 7.

2. Shape representation via signed distance functions

In [16, 18], Paragios et. al. represented a shape by the related signed distance function – a special level set function [15]. Specifically, given an object $\Omega \subset R^2$, which is assumed to be closed and bounded, then there is a unique viscosity solution to the following equation:

$$\mid \nabla \phi \mid = 1$$

$$\phi \begin{cases} > 0 & x \in \Omega \backslash \partial \Omega \\ = 0 & x \in \partial \Omega \\ < 0 & x \in R^2 \backslash \Omega. \end{cases} \quad (1)$$

Hence, any object in the plane corresponds to a unique signed distance function, and vice versa.

As a shape is invariant to translation, rotation and scaling, we may define an equivalent relation in the collection of objects in the plane. Any two objects are said to be *equivalent* if they have the same shape. Their signed distance functions are related. For example, let Ω_1 and Ω_2 be two objects with the same shape, and ϕ_1 and ϕ_2 be the signed distance functions respectively, then there exists a four-tuple (a, b, r, θ) such that:

$$\phi_2(x, y) = r\phi_1[\frac{(x - a)\cos\theta + (y - b)\sin\theta}{r},$$
$$\frac{-(x - a)\sin\theta + (y - b)\cos\theta}{r}], \quad (2)$$

where (a, b) represents the center, r the scaling factor and θ the angle of rotation. In this way, given any object, consequently a signed distance function, we may get the representation of other objects in the equivalence class by choosing the four-tuple (a, b, r, θ).

3. Cremers et al's segmentation model using shape priors and dynamic labelling

In this section, we review Cremers et al's segmentation model by using prior shapes and dynamic labelling.

In [3], Chan and Vese proposed a variational model based on a level set function, say ϕ, whose zero level set

segments the image domain into several intensity homogenous regions. The functional reads:

$$E(c_1, c_2, \phi) = \int_{\Omega} \{(u - c_1)^2 H(\phi) + (u - c_2)^2(1 - H(\phi))$$
$$+ \mu |\nabla H(\phi)|\} dx, \quad (3)$$

where $u : \Omega \to R$ is an image defined on Ω, c_1 and c_2 are two scalar variables, $H(x)$ is the Heaviside function:

$$H(x) = \begin{cases} 1, & x \geq 0 \\ 0, & x < 0, \end{cases} \quad (4)$$

and $\mu > 0$ is a parameter that describes how large the length of the boundaries is permitted, since the term $\int_{\Omega} |\nabla H(\phi)|$ just represents the length of zero level set of ϕ (see [14]).

In [5], Cremers et al. adopted Paragios et al.'s method [16] to represent a shape. Let ϕ be the level set function for segmentation, and ϕ_0 be the one embedding a given shape. Both are signed distance functions. Then their shape difference reads:

$$E_{shape}(\phi) = \int_{\Omega} (\phi - \phi_0)^2 dx. \quad (5)$$

Clearly, this integral means that the shape prior is enforced on the whole domain in Ω, which will allow the presence of objects in the background to affect the segmentation of the desired objects. Consequently, Cremers et al. introduced another function L, called *labelling* function, into the integral. The new shape term takes the form as follows:

$$E_{shape}(\phi, L) = \int_{\Omega} (\phi - \phi_0)^2 (L + 1)^2 dx, \quad (6)$$

where L defines the parts of the image domain Ω where the shape prior should be active. For example, the region where $L = -1$ will be excluded from the integral.

As for controlling the area of the region on which the shape prior is enforced and the regularity of the boundary separating the regions, an integral shape prior was developed by Cremers et al. as:

$$E_{shape}(\phi, L) = \int_{\Omega} \{(\phi - \phi_0)^2 (L + 1)^2 + \lambda^2 (L - 1)^2$$
$$+ \gamma |\nabla H(L)|\} dx. \quad (7)$$

In summary, Cremers et al.'s model is:

$$E(u_+, u_-, \phi, L) = E_{CV}(u_+, u_-, \phi) + \alpha E_{shape}(\phi, L), \quad (8)$$

where $\alpha > 0$ is a parameter.

Besides segmenting multiple independent objects in images, Cremers et al.'s model can also discriminate certain objects, e.g., whose shapes are similar to the prior shapes, from others by means of the labelling function. However,

this model does not allow for the translation, rotation and scaling of the prior shapes, i.e, the prior shapes have to be placed exactly at the locations of the desired objects, and also have the same poses and scales as these objects. These requirements are often not met in real applications.

4. Our Model

In this section, we detail our model. In section 4.1, our model on shape prior segmentation for an image with only one object is explained. Then in section 4.2, by introducing a labelling function, we extend the model to general cases where there are probably many objects in the image.

4.1. Shape prior segmentation for a simple case

Here, we consider a simple case where there is only one object inside the given image. Let $u : \Omega \to R$ be the given image defined on the domain Ω, ϕ a level set function for segmentation, and ψ a signed distance function for a given shape. As discussed in section 2, let ψ_0 be a fixed signed distance function for the shape, then ψ and ψ_0 are related by a four-tuple (a, b, r, θ) via the formula (2).

Instead of taking the shape comparison term as in [5], we define it as follows:

$$E_{shape}(\phi, \psi) = \int_{\Omega} (H(\phi) - H(\psi))^2 dx, \quad (9)$$

where $H(x)$ is the Heaviside function. This term is symmetric to ϕ and ψ, and independent of the size of the domain Ω. Moreover, it is unnecessary for ϕ to be a signed distance function.

Therefore, our model for shape prior segmentation can be written as:

$$E(c_1, c_2, \phi, \psi) = E_{CV}(c_1, c_2, \phi) + \lambda E_{shape}(\phi, \psi), \quad (10)$$

where $\lambda > 0$ is a parameter.

Due to the relation (2) between ψ and ψ_0, we may also write the functional in terms of ψ_0 by replacing ψ with (a, b, r, θ).

4.2. Shape prior segmentation for general cases

As stated in section 4.1, the shape comparison term (9) is defined on all the domain. Hence, it is inapplicable to general cases where there are multiple objects inside the given image, since other objects will contribute to the shape comparison. In this section, our model for the general cases is stated.

Besides the segmentation function ϕ and shape function ψ, we also introduce one more level set function L, called the *labelling* function in Cremers et al's work [5]. Then,

the prior shape will be compared with the region where both the level set function ϕ for segmentation and the labelling function L are positive. Consequently, instead of (9), the shape comparison term is defined as:

$$E_{shape}(\phi, L, \psi) = \int_{\Omega} (H(\phi)H(L) - H(\psi))^2 dx. \quad (11)$$

Here, $H(\phi)H(L)$ characterizes the intersection of $\{\phi > 0\}$ and $\{L > 0\}$. Ideally, the function L will segment from Ω a region inside which there is only the goal object.

Some restrictions are needed to control the labelling function L. First, if $\{(x, y) \in \Omega : L(x, y) > 0\}$ is empty, the shape comparison term (11) will exert no effect on the segmentation process. Therefore, the region in which L takes positive value should be as large as possible. Second, some regularity should be added to the boundary, i.e., the zero level set of L, by which L separates the domain Ω.

Thus, we revise (11) as follow:

$$E_{shape}(\phi, L, \psi) = \int_{\Omega} (H(\phi)H(L) - H(\psi))^2 dx$$
$$+ \mu_1 \int_{\Omega} (1 - H(L)) dx + \mu_2 \int_{\Omega} |\nabla H(L)| dx, \quad (12)$$

where $\mu_1 > 0$ and $\mu_2 > 0$ are two parameters. In this expression, the second term encourages the area of the region $\{(x, y) \in \Omega : L(x, y) > 0\}$, and the last one smoothes the boundary by which L separates the domain Ω.

However, it is elusive to choose an appropriate μ_1. Too large μ_1 will weaken the action of the labelling function because the region $\{L > 0\}$ will contain other objects besides the desirable object. On the other hand, if it is so small, L could be trapped at a state where the region $\{L > 0\}$ could be smaller than what it should be. Therefore, it is unlikely for the labelling function to control itself independently.

To overcome this difficulty, and noticing that when the ideal segmentation for the goal object is obtained, the reference shape function ψ should be also close to segment the object, we introduce an additional term as:

$$E_{\psi}(\psi, c_1, c_2) = \int_{\Omega} \{(u - c_1)^2 H(\psi) + (u - c_2)^2 (1 - H(\psi))\} dx, \quad (13)$$

where c_1 and c_2 are the same variables in Chan-Vese's model (3). Generally, this term will be small when the region $\{\psi > 0\}$ contains large regions occupied by objects and small regions of background. Therefore, the term prevents the reference shape from stopping at a smaller scale than the desirable object. Then, with the interaction between ψ and L in the shape comparison term (12), the labelling function L can be controlled less difficultly.

By combining all the above terms (3, 12, 13), our model can be written as:

$$E(\phi, \psi, L, c) = E_{CV} + E_{shape} + E_{\psi}, \quad (14)$$

or explicitly,

$$E = \int_\Omega (u-c_1)^2 H(\phi) + (u-c_2)^2(1-H(\phi))$$
$$+\lambda \int_\Omega (H(\phi)H(L) - H(\psi))^2$$
$$+\mu_1 \int_\Omega (1-H(L)) + \mu_2 \int_\Omega |\nabla H(L)|$$
$$+\nu \int_\Omega (u-c_1)^2 H(\psi) + (u-c_2)^2(1-H(\psi)),$$
(15)

where $c = (c_1, c_2)$, and λ, μ_1, μ_2 and ν are nonnegative parameters.

Remark 1: In this functional, we omit the length term in E_{CV}. It is partially because that the prior shape may control the smoothness of the zero level set of ϕ to some extend, and on the other hand, without the length term, a fast way for minimizing the functional can be developed, which will be discussed in the following section. However, even with length term, one can use the ideas in [19].

Remark 2: With the term E_ψ (13), the parameters μ_1 and μ_2 become easy to choose. In fact, we fix them for all the experiments listed in this paper.

Remark 3: Our model can also be easily extended to more general cases that permit affine transformations between the prior shapes and the desirable segmented objects instead of only orthogonal transformations discussed in this paper. These affine transformations will allow inexact matching of shapes, and make the model more robust.

5. Numerical algorithms

In this section, we discuss the numerical algorithms for minimizing the functionals presented in the last section. We first provide a proof of a fast solution principle, which was mentioned in [7] and is similar to Song and Chan's method [19], for minimizing Chan-Vese's segmentation model [3] without length term. We thus extend the principle to the minimization of our proposed functionals.

5.1. Numerical algorithms for the simple case

Recall the functional (10):

$$E(c, \phi, \psi) = \int_\Omega (u-c_1)^2 H(\phi) + (u-c_2)^2(1-H(\phi))$$
$$+\lambda \int_\Omega (H(\phi) - H(\psi))^2.$$

Here, we omit the length term in the Chan-Vese's model.

Then, similarly as Chan-Vese's method in [3], the minimization of functional (10) is performed by solving the following equations (16) $\sim$(21):

$$c_1 = \frac{\int_\Omega u H(\phi) dx dy}{\int_\Omega H(\phi) dx dy},$$

$$c_2 = \frac{\int_\Omega u(1-H(\phi)) dx dy}{\int_\Omega (1-H(\phi)) dx dy}, \tag{16}$$

and for the shape function ψ, the gradient descents with respect to the four-tuple (a, b, r, θ) are given as follows:

$$\frac{\partial a}{\partial t} = \int_\Omega (H(\psi) - H(\phi))\{\psi_{0x}(x^*, y^*)\cos\theta$$
$$-\psi_{0y}(x^*, y^*)\sin\theta\}\delta(\psi) dx dy, \tag{17}$$

$$\frac{\partial b}{\partial t} = \int_\Omega (H(\psi) - H(\phi))\{\psi_{0x}(x^*, y^*)\sin\theta$$
$$+\psi_{0y}(x^*, y^*)\cos\theta\}\delta(\psi) dx dy, \tag{18}$$

$$\frac{\partial r}{\partial t} = \int_\Omega (H(\psi) - H(\phi))\{-\psi_0(x^*, y^*)$$
$$+\psi_{0x}(x^*, y^*)x^* + \psi_{0y}(x^*, y^*)y^*\}\delta(\psi) dx dy, \tag{19}$$

$$\frac{\partial \theta}{\partial t} = \int_\Omega (H(\psi) - H(\phi))\{-r\psi_{0x}(x^*, y^*)y^*$$
$$+r\psi_{0y}(x^*, y^*)x^*\}\delta(\psi) dx dy, \tag{20}$$

where ψ_0 is a fixed signed distance function representing the given shape, and ψ is related to ψ_0 via (2), and

$$x^* = \frac{(x-a)\cos\theta + (y-b)\sin\theta}{r},$$

$$y^* = \frac{-(x-a)\sin\theta + (y-b)\cos\theta}{r},$$

$$\psi_{0x} = \frac{\partial\psi_0}{\partial x}, \qquad \psi_{0y} = \frac{\partial\psi_0}{\partial y},$$

and for the segmentation function ϕ,

$$\frac{\partial \phi}{\partial t} = -\{(u-c_1)^2 - (u-c_2)^2$$
$$+2\lambda(H(\phi) - H(\psi))\}\delta(\phi), \tag{21}$$

where $\delta(x)$ is the derivative of the Heaviside function $H(x)$ in the distribution sense.

In summary, for each iteration in the experiment, as in [3], we can update c_1, c_2, ψ and ϕ one by one according to formulas (16) ∼(21).

However, due to the fact that we only need the sign of the segmentation function ϕ, we will update it instead of using formula (21) but the following principle:

$$\phi = \begin{cases} 1, & A(\phi, \psi, c) \geq 0; \\ -1, & A(\phi, \psi, c) < 0. \end{cases} \qquad (22)$$

where $A(\phi, \psi, c) = -\{(u - c_1)^2 - (u - c_2)^2 + 2\lambda(H(\phi) - H(\psi))\}$.

This principle will accelerate the minimization process remarkably. This is because this principle only cares about the sign of ϕ (through $H(\phi)$), and it thus saves lots of computational time which is wastefully spent in updating the value of ϕ instead of its sign by using (21). This idea can be found in [7, 19].

In the following theorem, we prove that the above principle is equivalent to the conventional gradient descent method on the Euler-Lagrange equation if we minimize Chan-Vese's functional without length term [3]. We thus provide another proof for Song-Chan's one step convergence theorem [19].

Without length term, Chan-Vese's functional reads:

$$E(c_1, c_2, \phi) = \int_\Omega \{(u - c_1)^2 H(\phi) \\ + (u - c_2)^2 (1 - H(\phi))\} dx, \quad (23)$$

and the Euler-Lagrange equation for updating ϕ is:

$$\frac{\partial \phi}{\partial t} = -[(u - c_1)^2 - (u - c_2)^2]\delta(\phi), \qquad (24)$$

and c_1, c_2 are given by (16), (16).

In this case, the fast solution principle becomes:

$$\phi = \begin{cases} 1, & -[(u - c_1)^2 - (u - c_2)^2] \geq 0; \\ -1, & -[(u - c_1)^2 - (u - c_2)^2] < 0. \end{cases} \quad (25)$$

Then, we have the following theorem.

Theorem 1. *Let $u : \Omega \to R$ be a binary image defined on the domain Ω, for simplicity, denoted as $u = \chi_A(x, y)$, where χ_A is the characteristic function of $A \subseteq \Omega$, and $\phi: \Omega \times \{t \geq 0\} \to R$ be the segmentation function. Then the minimization of the Chan-Vese's functional by performing (16), (16) and (24) will be equivalent to the procedure by performing (16), (16) and the principle (25).*

Proof. For convenience, let us replace c_1, c_2 by $c_1(t)$, $c_2(t)$ in expressions (16), (16) and (24). And without loss of generality, suppose $c_1(0) > c_2(0)$, which are derived from (16) and (16) with the initial segmentation function $\phi(x, y, 0)$.

We claim that: by performing (16), (16) and (24), the term $(u - c_1(t))^2 - (u - c_2(t))^2$ will keep the sign.

In fact, the amount $(c_1(t) - c_2(t))^2$ will be non-decreasing as $t \to \infty$. This is because:

$$\begin{aligned} \frac{dc_1}{dt} &= \frac{1}{\int_\Omega H(\phi)}[\int_\Omega u\delta(\phi)\phi_t - c_1(t)\int_\Omega \delta(\phi)\phi_t] \\ &= \frac{1}{\int_\Omega H(\phi)}\int_\Omega (u - c_1(t))\delta(\phi)\phi_t \\ &= \frac{1}{\int_\Omega H(\phi)}\int_\Omega (u - c_1(t))\delta(\phi)[-(u - c_1(t))^2 \\ &\quad + (u - c_2(t))^2]\delta(\phi), \end{aligned} \qquad (26)$$

then, if $c_2(t) < c_1(t)$, thus, $0 \leq c_2(t) < c_1(t) \leq 1$, it is easy to check that:

$$(u - c_1(t))[-(u - c_1(t))^2 + (u - c_2(t))^2] > 0, \quad (27)$$

whenever u takes value 1 or 0. Therefore, $dc_1/dt \geq 0$. On the other hand, if $c_2(t) \geq c_1(t)$, we have $dc_1/dt \leq 0$. Consequently,

$$(c_1(t) - c_2(t))\frac{dc_1}{dt} \geq 0, \qquad (28)$$

similarly,

$$(c_1(t) - c_2(t))\frac{dc_2}{dt} \leq 0. \qquad (29)$$

Combining (28) and (29), we have:

$$\frac{d(c_1(t) - c_2(t))^2}{dt} \geq 0,$$

that is, the amount $(c_1(t) - c_2(t))^2$ is non-decreasing.

By the assumption, $c_1(0) > c_2(0)$, we may arrive that: $c_1(t) > c_2(t)$ for any $t > 0$. Consequently, the term $(u - c_1(t))^2 - (u - c_2(t))^2$ will keep the sign as $t \to \infty$.

Recall (24):

$$\frac{\partial \phi}{\partial t} = -[(u - c_1)^2 - (u - c_2)^2]\delta(\phi).$$

Since the right side will never change sign, i.e., the sign is the same as the sign of $-[(u - c_1(0))^2 - (u - c_2(0))^2]$. Therefore, if $-[(u - c_1(0))^2 - (u - c_2(0))^2] > 0$ at point $(x, y) \in \Omega$, $\phi(x, y, t)$ will be positive as $t \to \infty$, otherwise $\phi(x, y, t)$ will be negative as $t \to \infty$. This is just the principle (25). □

Remark 4: The theorem shows that it is reasonable to use (22) to minimize the functional (10) to some extend. On the other hand, it will be unavoidable to see some fuzzy boundaries during the evolution if we apply the principle to very noise images. In this case, we prefer to use the conventional way with the length term.

5.2. Numerical algorithms for the general case

We now return to discuss the numerical algorithms for the functional (15). Similarly as discussed in the previous section, we update c_1, c_2, L, ψ and ϕ for each iteration in the experiments as follows:

$$c_1 = \frac{\int_\Omega u(H(\phi) + \nu H(\psi))dxdy}{\int_\Omega (H(\phi) + \nu H(\psi))dxdy}, \qquad (30)$$

$$c_2 = \frac{\int_\Omega u((1 - H(\phi)) + \nu(1 - H(\psi)))dxdy}{\int_\Omega ((1 - H(\phi)) + \nu(1 - H(\psi)))dxdy}, (31)$$

and

$$\frac{dL}{dt} = -\lambda H(\phi)(1 - 2H(\psi))|\nabla L| + \mu_1|\nabla L|$$
$$+\mu_2|\nabla L|\nabla \cdot (\frac{\nabla L}{|\nabla L|}). \qquad (32)$$

As for the shape function ψ, we replace the term $(H(\psi) - H(\phi))$ in (17)$\sim$(20) by the following one:

$$2\lambda(H(\psi) - H(\phi)H(L)) + \nu[(u - c_1)^2 - (u - c_2)^2], (33)$$

and

$$\frac{d\phi}{dt} = -\delta(\phi)\{[(u - c_1)^2 - (u - c_2)^2]$$
$$+2\lambda H(L)(H(\phi)H(\psi) - H(L))\}. \quad (34)$$

To speed up the minimization process, instead of (34), we update ϕ with the principle similar to (22), which reads:

$$\phi = \begin{cases} 1, & A(\phi, \psi, L, c) \geq 0; \\ -1, & A(\phi, \psi, L, c) < 0. \end{cases} \qquad (35)$$

where $A(\phi, \psi, L, c) = -\{[(u - c_1)^2 - (u - c_2)^2] + 2\lambda H(L)(H(\phi)H(\psi) - H(L))\}$.

Moreover, we use local level set method, which was proposed by Peng et al. in [17], to update the labelling function L, e.g., we only calculate L in a tube around its zero level set instead of the whole domain Ω. All these techniques make the minimization process much more faster than the conventional gradient descent method.

6. Experiment results

In this section, we only present experimental results for the general cases (section 4.2) since the simple case (section 4.1) can be included in the general ones. Here, we show the results for two real images. One is a hand occluded by other objects (Figure 1) and the other is the same hand with some missing parts (Figure 2). The prior shape is a similar hand.

To view the segmentation process clearly, we list three states (initial, middle and final) for each function: segmentation function ϕ, labelling function L, shape function ψ and the *goal* segmentation which is represented by the boundary of the region $\{\phi > 0\} \bigcap \{L > 0\}$. Specifically, for each result, the first row lists the original image and the prior shape; from the second row to the fourth row, each column respectively represents the initial, middle and final states of the segmentation function ϕ, labelling function L, shape function ψ, and the goal segmentation which is represented by the boundary of the region $\{\phi > 0\} \bigcap \{L > 0\}$.
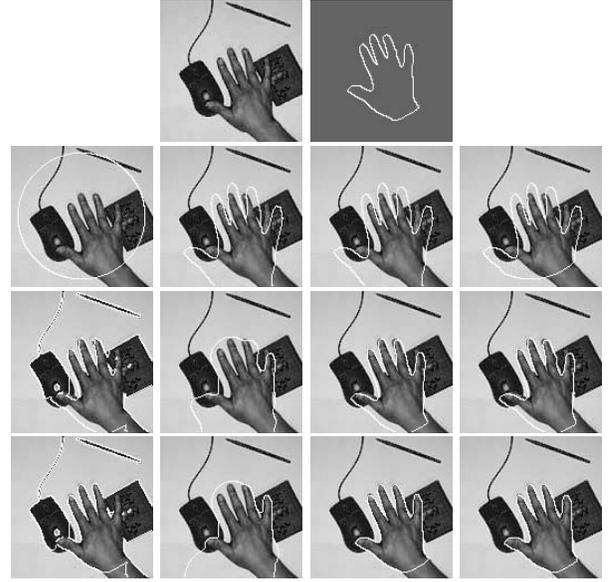

Figure 1. The first row lists the original image and the prior shape. From the second row to the fourth row, each column respectively represents the initial, middle and final step of the segmentation function ϕ, labelling function L, shape function ψ, and the goal segmentation which is represented by the boundary of the region $\{\phi > 0\} \bigcap \{L > 0\}$. In this experiment, the parameters chosen are: $\lambda = 3.0$, $\mu_1 = 0.2$, $\mu_2 = 0.2$, $\nu = 2.0$. This example verifies that our model can capture an object occluded by other ones via the supervision of the prior shape from a real image.

From these two examples (Figure 1 and Figure 2), besides the segmentation of the desirable object, we also find that the *labelling* function successfully separates the desirable region from the other region in the image domain. These results demonstrate that our model can segment an object whose shape is similar to the prior shape from an image even though the object is occluded by other ones (Figure 1) or has some missing parts (Figure 2).
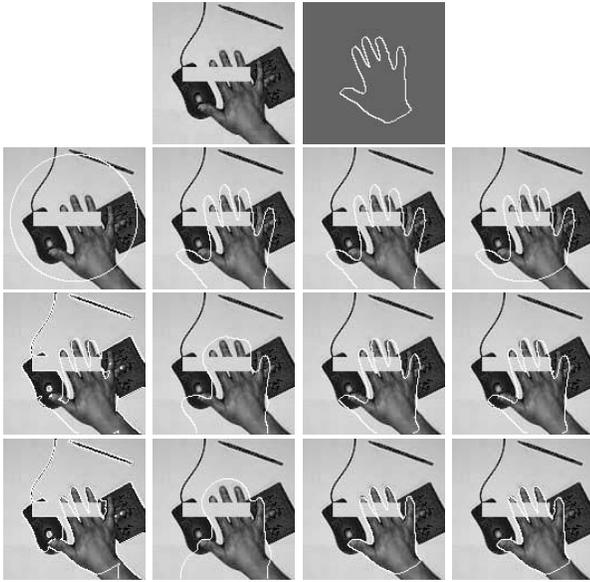
Figure 2. The first row lists the original image and the prior shape. From the second row to the fourth row, each column respectively represents the initial, middle and final step of the segmentation function ϕ, labelling function L, shape function ψ, and the goal segmentation which is represented by the boundary of the region $\{\phi > 0\} \bigcap \{L > 0\}$. In this experiment, the parameters chosen are: $\lambda = 2.0$, $\mu_1 = 0.2$, $\mu_2 = 0.2$, $\nu = 2.0$. This example shows that our model can also be applied to segment an object similar to the prior shape by filling in the missing parts from a real image.

7. Conclusion

In this paper, we propose a level set based variational model for segmentation using prior shapes. Inspired by Cremers' work [5], we also introduce a labelling function which, together with the level set function for segmentation, dynamically indicates the region with which the prior shape should be compared. Our model is capable of segmenting an object from an image based on the image intensity as well as the prior shape. The proposed model permits translation, scaling and rotation of the prior shape. In addition, a fast way is established for the minimization of our functionals.

References

[1] L. Ambrosio and V. Tortorelli. Approximation of functionals depending on jumps by elliptic functionals via gamma convergence. *Comm. Pure Appl. Math.*, 43:999–1036, 1990.

[2] V. Caselles, R. Kimmel, and G. Sapiro. Geodesic active contours. *Int. J. of Computer Vision*, 22(1):61–79, 1997.

[3] T. Chan and L. Vese. Active contours without edges. *IEEE Transaction on Image Processing*, 10(2):266–277, Feb. 2001.

[4] Y. Chen, H. Tagare, S. Thiruvenkadam, F. Huang, D. Wilson, K. Gopinath, R. Briggs, and E. Geiser. Using prior shapes in geometric active contours in a variational framework. *Int. J. of Computer Vision*, 50(3):315–328, 2002.

[5] D. Cremers, N. Sochen, and C. Schnorr. Towards recognition-based variational segmentation using shape priors and dynamic labeling. *In L. Griffith, editor, Int. Conf. on Scale Space Theories in Computer Vsion*, volume 2695 of LNCS:388–400, Isle of Skye, 2003, Springer.

[6] D.Cremers, F. Tischhauser, J. Weickert, and C. Schnorr. Diffusion snakes: introducing statistical shape knowledge into the mumford-shah functional. *Int. J. of Computer Vision*, 50(3):295–313, 2002.

[7] F. Gibou and R. Fedkiw. Fast hybrid k-means level set algorithm for segmentation. *http://math.stanford.edu/ fgibou/*.

[8] M. Kass, A. Witkin, and D. Terzopoulos. Snakes: Active contour models. *Int. J. of Computer Vision*, 1:321–331, 1987.

[9] M. Leventon, O. Faugeraus, W. Grimson, and W. W. III. Level set based segmentation with intensity and curvature priors. *Mathematical Methods in Biomedical Image Analysis*, 2000.

[10] M. Leventon, W. Grimson, and O. Faugeraus. Statistical shape influence in geodesic active contours. *CVPR*, pages 316–323, 2000.

[11] R. Malladi, J. Sethian, and B. Vemuri. Shape modeling with front propagation: A level set approach. *IEEE Trans. on PAMI*, 17(2):158–175, 1995.

[12] J. Morel and S. Solimini. *Variational methods in image segmentation*. Birkhauser, Boston, 1995.

[13] D. Mumford and J. Shah. Optimal approximation by piecewise smooth functions and associated variational problems. *Comm. Pure Appl. Math.*, 42:577–685, 1989.

[14] S. Osher and R. Fedkiw. Level set methods: an overview and some recent results. *J. Comput. Phys*, 169(2):463–502, 2001.

[15] S. Osher and J. Sethian. Fronts propagating with curvature dependent speed algorithm based on hamilton-jacobi formulations. *J. Comput. Phys*, 79:12–49, 1988.

[16] N. Paragios, M. Rousson, and V. Ramesh. Matching distance functions: A shape-to-area variational approach for global-to-local registration. *ECCV, Copenhangen, Denmark*, 2002.

[17] D. Peng, B. Merriman, S. Osher, H. Zhao, and M. Kang. A pde-based fast local level set method. *J. Comput. Phys*, 155:410–438, 1999.

[18] M. Rousson and N. Paragios. Shape priors for level set representaions. *ECCV, Copenhangen, Denmark*, 2002.

[19] B. Song and T. Chan. A fast algorithm for level set based optimization. *UCLA CAM Report 02-68*, 2002.

[20] A. Tsai, A. Yezzi, W. Wells, C. Tempany, D. Tucker, A. Fan, E. Grimson, and A. Willsky. Model-based curve evolution technique for image segmentation. *CVPR*, pages 463–468, 2001.